Journal of Applied Mechanics and Technical Physics, Vol. 40, No. 5, 1999

A STUDY OF HEAT-TRANSFER PROCESSES IN A SUPERSONIC FLOW AROUND A SPHERICALLY BLUNTED CONE WITH ALLOWANCE FOR INJECTION OF A GAS-COOLER

V. I. Zinchenko and A. Ya. Kuzin

UDC 536.24.01

The heat- and mass-transfer processes of a spherically blunted cone and a supersonic air flow are identified by the methods of solving direct and inverse problems with allowance for the heat flow along the contour and the injection of a gas-cooler. The ranges of applicability of the standard one-dimensional approaches and the method of a thin wall for recovering heat fluxes directed toward the body in flow are shown in the entire time period considered.

In a supersonic flow around aircrafts, the heat flow along the contour and the injection of a gas-cooler from the surface are effective means for decreasing the surface temperature in the region of large heat loads [1–4]. The solution of conjugate [5, 6] and inverse [7, 8] heat-conduction problems is widely used to determine the heat flux and the temperature. The combined solution of the direct (DHCP) and inverse heat-conduction problems (IHCP) in a two-dimensional formulation increases the reliability of results and provides insight into the processes under study. Regularized numerical methods are preferred in solving multidimensional nonlinear IHCP that involve the injection and the complex geometry of aircrafts [9]. In the publication [9] devoted to recovery of heat fluxes in a supersonic flow around a spherically blunted cone, Zinchenko and Kuzin showed the need to solve IHCP for a number of materials in regions where the heat flux $q_w(s)$ changes substantially along the generatrix. In the presence of gas injection from a limited part of the surface, this behavior of $q_w(s)$ is observed in the region behind the injection section where a heat-shield regime is realized, which corresponds, under certain conditions, to the maximum heat fluxes and surface temperatures. Therefore, one needs to use models that take into account the heat flow along the generatrix and estimates of the standard one-dimensional approaches to solve the inverse problem of recovery of the heat flux and the surface temperature.

In the present paper, the solution of the identification problem of heat-transfer processes in a supersonic air flow around a spherically blunted cone is considered with account of the heat flow along the contour and the injection of a gas-cooler from a spherically blunted surface. The effect of the thermophysical properties of the material, the intensity of the injected-gas flow rate, and the two-dimensionality of heat-transfer processes on the parameters of the nonstationary heat transfer are studied by the methods of solving direct and inverse heat-conduction problems.

1. Physical and Mathematical Formulation of Direct and Inverse Problems. The heating of a spherically blunted hollow cone in an axisymmetric supersonic air flow is considered. In describing heat-transfer processes in a porous spherical shell with allowance for the assumption that the filtration of the gas injected toward the surface is one-dimensional, one can use the energy-conservation equation in the natural coordinate system

$$R_N^2 \rho_1 c_1 (1-\varphi) \frac{\partial T}{\partial t} = \frac{1}{H_1 r}\left[\frac{\partial}{\partial \xi}\left(\frac{r}{H_1}\lambda_1(1-\varphi)\frac{\partial T}{\partial \xi}\right) + \frac{\partial}{\partial n}\left(rH_1\lambda_1(1-\varphi)\frac{\partial T}{\partial n}\right)\right]$$

State University of Tomsk, Tomsk 634050. Translated from Prikladnaya Mekhanika i Tekhnicheskaya Fizika, Vol. 40, No. 5, pp. 123–132, September–October, 1999. Original article submitted July 1, 1997; revision submitted November 3, 1997.

 0021-8944/99/4005-0886 $22.00

$$+(\rho v)_w \frac{R_N r_w}{r H_1} c_{pg} \frac{\partial T}{\partial n} \qquad \left(0 < n < \frac{L}{R_N}, \quad 0 < \xi \leqslant \xi_1\right). \tag{1.1}$$

For the conical section of a body, the heat-conduction equation has the form

$$R_N^2 \rho_2 c_2 \frac{\partial T}{\partial t} = \frac{1}{r}\left[\frac{\partial}{\partial \xi}\left(r\lambda_2 \frac{\partial T}{\partial \xi}\right) + \frac{\partial}{\partial n}\left(r\lambda_2 \frac{\partial T}{\partial n}\right)\right] \qquad \left(0 < n < \frac{L}{R_N}, \quad \xi_1 < \xi < \xi_b\right). \tag{1.2}$$

The initial and boundary conditions are written in the form

$$T(0, \xi, n) = T_{\text{in}}(\xi, n), \qquad 0 \leqslant n \leqslant L/R_N, \qquad 0 \leqslant \xi \leqslant \xi_b; \tag{1.3}$$

$$[(\alpha/c_p)_1 (H_r - h_w)]\Big|_{n=-0} - \varepsilon\sigma T_w^4\Big|_{n=-0} = -\frac{\lambda_1(1-\varphi)}{R_N} \frac{\partial T}{\partial n}\Big|_{n=+0}, \quad 0 \leqslant \xi \leqslant \xi_1; \tag{1.4}$$

$$[(\alpha/c_p)_2 (H_r - h_w)]\Big|_{n=-0} - \varepsilon\sigma T_w^4\Big|_{n=-0} = -\frac{\lambda_2}{R_N} \frac{\partial T}{\partial n}\Big|_{n=+0}, \quad \xi_1 < \xi \leqslant \xi_b; \tag{1.5}$$

$$\frac{\lambda_1(1-\varphi)}{R_N} \frac{\partial T}{\partial n}\Big|_{n=L/R_N} = (\rho v)_w c_{pg} \frac{r_w}{(rH_1)_{w1}} (T_g - T_{w1}), \quad 0 \leqslant \xi \leqslant \xi_1; \tag{1.6}$$

$$\frac{\partial T}{\partial n}\Big|_{n=L/R_N} = 0, \qquad \xi_1 < \xi \leqslant \xi_b; \tag{1.7}$$

$$\frac{\partial T}{\partial \xi}\Big|_{\xi=0} = 0; \tag{1.8}$$

$$\frac{\lambda_1(1-\varphi)}{H_1} \frac{\partial T}{\partial \xi}\Big|_{\xi=\xi_1-0} = \lambda_2 \frac{\partial T}{\partial \xi}\Big|_{\xi=\xi_1+0}; \tag{1.9}$$

$$\frac{\partial T}{\partial \xi}\Big|_{\xi=\xi_b} = 0. \tag{1.10}$$

In Eqs. (1.1)-(1.10), T is the temperature, $n = \bar{n}/R_N$, $\xi = s/R_N$ are the transverse and longitudinal nondimensional spatial coordinates, t is the time, $r = (r_w/R_N) - n\cos(\pi/2 - \xi)$, $H_1 = 1 - n$ are the Lamé coefficients, R_N is the spherical bluntness radius, L is the shell thickness, $\xi_1 = \pi/2 - \beta$ (β is the cone angle), $r_w/R_N = \sin\xi$ for the spherical section and $r_w/R_N = \sin\xi_1 + (\xi - \xi_1)\sin\beta$ for the conical section, ρ is the density, c_{pg} is the coefficient of specific heat capacity of the gas, c is the coefficient of specific heat capacity of the solid, λ is the heat conductivity, α is the heat-transfer coefficient, $(\rho v)_w$ is the gas-cooler flow rate, φ is the porosity, H_r is the recovery enthalpy, h_w is the gas enthalpy on the wall, ε is the emissivity factor, and σ the Stefan-Boltzmann constant.

The subscripts w and $w1$ refer to the quantities at the shell surface $n = 0$ and the inner surfaces of the shell, respectively, the subscripts 1 and 2 refer to the thermophysical characteristics of the spherical and conical sections, respectively, the subscript g refers to the gaseous phase of the porous spherical shell, and the subscripts "in" and "fin" refer to the initial and final states.

In the boundary layer, we consider the mixed flow regime: laminar at the porous spherical shell in the vicinity of the stagnation point and turbulent in the remaining section of the spherical shell and the cone. The standard model of a pointwise laminar–turbulent transition is used; the transition point is given with account of the results of the parametric calculations of the heating problem for the shell, which were performed in the conjugate formulation where exact boundary-layer equations were used in the gaseous case [3].

Provided the air is injected into the incoming flux, the heat-transfer coefficients are determined by the formula [10]

$$(\alpha/c_p)_1 = (\alpha/c_p)_1^0 \exp\left(-\zeta_0 \frac{(\rho v)_w(\xi)}{(\alpha/c_p)_1^0(\xi)}\right), \tag{1.11}$$

where $(\alpha/c_p)_1^0$ is the heat-transfer coefficient in the absence of injection, ζ_0 is a coefficient equal to 0.37 and 0.6 for the laminar and turbulent regimes, respectively.

In the shielded zone of the conical section, with allowance for the treatment suggested in [11] the heat-transfer coefficient takes the form

$$(\alpha/c_p)_2 = (\alpha/c_p)_2^0(1 - \zeta_1 b^{\zeta_2}). \tag{1.12}$$

Here $(\alpha/c_p)_2^0$ is the heat-transfer coefficient in the absence of injection, b is a nondimensional parameter that characterizes the ratio of the total mass of the injected gas to the product of the heat-transfer coefficient for the cross section z in the absence of injection by the cone surface area from z_1 to the current value of z (z is the axial cylindrical coordinate), and ζ_1 and ζ_2 are constants determined from a comparison with the results of solution of the conjugate problem [3].

If the law of gas flow rate for a sphere is taken in the form

$$(\rho v)_w(\xi) = (\rho v)_w(0)(1 + a\sin^2\xi) \qquad (a = \text{const}),$$

we have

$$b = \frac{2(\rho v)_w(0)[1 - \cos\xi_1 + a(2/3 - \cos\xi_1 + (1/3)\cos^3\xi_1)]}{(z - z_1)(\cos\beta)^{-1}[2\sin(\pi/2 - \beta) + \tan\beta(z - z_1)](\alpha/c_p)_2^0}.$$

In the absence of injection, the heat-transfer coefficients are determined with the use of the data from [12]. On the spherical section, we have

$$(\alpha/c_p)_1^0(\xi) = (0.55 + 0.45\cos 2\xi)(\alpha/c_p)_1^0(0), \qquad (\alpha/c_p)_1^0(0) \approx 1.05U_\infty^{1.08}(\rho_\infty/R_N)^{0.5}, \tag{1.13}$$

for the laminar-flow rate regime and

$$\begin{aligned}(\alpha/c_p)_1^0(\xi) &= (3.75\sin\xi - 3.5\sin^2\xi)(\alpha/c_p)_1^0(\xi_*)\\ (\alpha/c_p)_1^0(\xi_*) &\approx 16.4U_\infty^{1.25}\rho_\infty^{0.8}R_N^{-0.2}(1 + h_w/H_{e0})^{-2/3}\end{aligned} \tag{1.14}$$

for the turbulent-flow regime.

On the conical section, we have

$$(\alpha/c_p)_2^0(\xi) = 2.2(P_e/P_{e0})(u_e/v_m)k^{-0.4}(r_w/R_N)^{-0.2}(\alpha/c_p)_1^0(\xi_*) \tag{1.15}$$

for the turbulent-flow regime.

The value of H_r is determined by the formula

$$H_r = H_{e0}[(P_e/P_{e0})^{(\gamma-1)/\gamma} + \sqrt{\Pr}(u_e/v_m)^2] \tag{1.16}$$

for the laminar-flow regime and by the formula

$$H_r = H_{e0}[(P_e/P_{e0})^{(\gamma-1)/\gamma} + \sqrt[3]{\Pr}(u_e/v_m)^2] \tag{1.17}$$

for the turbulent-flow regime.

For a sphere, the pressure distribution over the body surface referred to the value of the deceleration pressure is found by the formula [13]

$$(P_e/P_{e0})(\xi) = 1 - 1.17\sin^2\xi + 0.225\sin^6\xi \tag{1.18}$$

for a sphere, and it is taken from the table of [14] for a cone. The air enthalpy at the surface is $h_w = 965.5T_w + 0.0735T_w^2$.

In Eqs. (1.13)–(1.17), the following values are used: $H_{e0} = h_\infty[1 + (\gamma - 1)\mathrm{M}_\infty^2/2]$, $u_e/v_m = \sqrt{1 - (P_e/P_{e0})^{(\gamma-1)/\gamma}}$, $v_m = \sqrt{2H_{e0}}$, and $k = (\gamma - 1 + 2/\mathrm{M}_\infty^2)/(\gamma + 1)$; here U_∞ [km/sec] is the motion velocity, ρ_∞ [kg/m^3] is the density in the incoming flow, R_N [m] is the spherical bluntness radius, γ is the adiabatic exponent, M is the Mach number, Pr is the Prandtl number; the subscripts e and $e0$ refer to the quantities at the outer frontier of the boundary layer and the outer frontier at the stagnation point, and the subscript ∞ refers to those in the incoming flow.

The two-dimensional direct problem is to find the temperature field $T(\xi, n, t)$ in the domain $\bar{D} = \{(\xi, n, t)\colon 0 \leqslant \xi \leqslant \xi_b, 0 \leqslant n \leqslant L/R_N, 0 < t \leqslant t_{\text{fin}}\}$ satisfying Eqs. (1.1) and (1.2), the initial and boundary

conditions (1.3)–(1.10) with relations (1.11)–(1.18).

If the convective heat flux from the gaseous phase $q_w(\xi,t) = (\alpha/c_p)(H_r - h_w)$ is not known and one needs to find this flux and the temperature field $T(\xi,n,t)$ in the domain $D = \{(\xi,n,t)\colon 0 \leqslant \xi \leqslant \xi_b, 0 \leqslant n < L/R_N, 0 < t \leqslant t_{\text{fin}}\}$ according the known additional condition

$$T(\xi, L/R_N, t) = T_{w1}(\xi,t), \tag{1.19}$$

we have the formulation of the two-dimensional boundary IHCP. The total heat flux to a solid body $Q_w(\xi,t) = q_w - \varepsilon\sigma T_w^4$ is found by means of the found heat flux $q_w(\xi,t)$ and temperature $T_w(\xi,t)$.

2. Algorithms for Solving Direct and Inverse Problems. Similarly to [9], we use the method of splitting over the spatial variables n and ξ to solve the two-dimensional DHCP. The one-dimensional equations obtained by splitting are solved by the iteration-interpolation method [5, 8] with iterations over the coefficients. Iterations are terminated upon reaching the required accuracy in determining the temperature.

For conveniently presenting the algorithm for solving the two-dimensional IHCP, Eqs. (1.1) and (1.2) are given in the general form

$$\frac{\partial}{\partial\xi}\left(F_\xi \frac{\partial T}{\partial\xi}\right) + \frac{\partial}{\partial n}\left(F_n \frac{\partial T}{\partial n}\right) = -K\frac{\partial T}{\partial n} + C\frac{\partial T}{\partial t}, \tag{2.1}$$

where the form of the coefficients F_ξ, F_n, K, and C is determined by the formulation of the problem.

To find the temperature in the $(l,\ k)$th spatial node, the recurrence relation

$$B^j_{l,k}T^j_{l,k} = F^j_{l,k} \qquad (l = \overline{0,L}, \qquad j = \overline{1,M}) \tag{2.2}$$

is obtained approximating the derivatives from [15].

Here

$$B^j_{l,k} = \frac{F^j_{nl,k+1} + F^j_{nl,k}}{2h_n^2} - \frac{K^j_{l,k+1}}{2h_n}; \qquad F^j_{l,k} = C^j_{l,k+1}\frac{T^j_{l,k+1} - T^{j-1}_{l,k+1}}{h_t}$$

$$- \frac{(F^j_{nl,k+2} + F^j_{nl,k+1})(T^j_{l,k+2} - T^j_{l,k+1}) - F^j_{nl,k+1} - F^j_{nl,k}}{2h_n^2} - \frac{K^j_{l,k+1}T^j_{l,k+2}}{2h_n} - \left[\frac{\partial}{\partial\xi}\left(F_\xi\frac{\partial T}{\partial\xi}\right)\right]^j_{l,k+1}.$$

In calculating the derivative with respect to ξ, the step h_ξ was taken variable in the nodes of the differential grid and conditions (1.8) and (1.10) are taken into account at the boundaries of the region $\xi = 0$ and $\xi = \xi_b$. Here and below, L, K, and M are the number of nodes of the differential grid with respect to ξ, n, and t, and h_ξ, h_n, and h_t are the appropriate steps over these variables.

The nonlinear relation (2.2) is used for finding the temperature at the kth spatial line with the use of the known temperature values at the $(k+1)$th and $(k+2)$th lines. The resulting value is refined by iterations over the coefficients. The known temperature value at the $(k+1)$th line is used as the initial approximation. The calculation begins with finding the temperature value at the $(K-2)$th line. The temperature value at the Kth line is given by the experimental function $T_{w1}(\xi,t)$ from (1.19), and it is determined from the finite-difference analog of conditions (1.6) and (1.7) at the $(K-1))$th line. Using relation (2.2) successively for the $(K-2)$, $(K-3),\ldots$, and zeroth lines, we find the temperature field for the entire region $\bar{D}$ and the total heat flux $Q_w(\xi,t)$.

This method of solving IHCP is referred to the class of direct numerical methods (DNM) [7]. The steps over spatial variables and time are used here as the natural regularization parameters. The potentialities of the DNM are substantially extended if the interpolation and approximation of one- and two-dimensional cubic splines [16], smoothing, etc., are used primarily for processing of the initial data and for calculations.

If necessary, the DNM supplement well the regularized numerical methods [15]. In this case, the algorithm of calculation is constructed as follows. In finding the temperature value on the kth spatial line, staged regularization over t and ξ is performed. At the first stage, for Eq. (2.2) Tikhonov's functional is

written in the form

$$\Psi^j_{l,k}(\alpha) = \sum_{j=1}^{M}(B^j_{l,k}T^j_{l,k} - F^j_{l,k})^2 + \frac{\alpha k_1}{h_t^2}\sum_{j=1}^{M}(T^j_{l,k} - T^{j-1}_{l,k})^2 + \frac{\alpha k_2}{h_t^4}\sum_{j=1}^{M}(T^{j+1}_{l,k} - 2T^j_{l,k} + T^{j-1}_{l,k})^2 \quad (l = \overline{0, L}). \tag{2.3}$$

After minimization of Eq. (2.3) over all $T^j_{l,k}$ ($j = \overline{1, M}$), for finding the temperature in the (l, k)th spatial node, we obtain a system of nonlinear algebraic equations with a symmetric five-diagonal, positively defined matrix, whose coefficients are given in [15]. The system is solved by the method of nonmonotonic sweep with iterations over the coefficients. The known temperature in the $(l, k+1)$th spatial node is used as the preliminary approximation. The iteration process is completed when the required accuracy of determining the temperature is attained. This procedure is successively used for finding the temperature in all the nodes of the kth line.

At the second stage, Tikhonov's functional is used in the form

$$\Omega^j_{l,k}(\alpha) = \sum_{l=0}^{L}(B^j_{l,k}T^j_{l,k} - F^j_{l,k})^2 + \alpha k_3 \sum_{l=0}^{L-1}(T^j_{l+1,k} - T^j_{l,k})/h^2_{\xi l} + 4\alpha k_4 \sum_{l=0}^{L}[T^j_{l+1,k}h_{\xi l-1}/h_{\xi l}$$

$$-T^j_{l,k}(1 + h_{\xi l-1}/h_{\xi l}) + T^j_{l-1,k}]^2 h^{-2}_{\xi l-1}(h_{\xi l-1} + h_{\xi l})^{-2} \qquad (j = \overline{1, M}). \tag{2.4}$$

In the functionals (2.3) and (2.4), α is the regularization parameter and k_1, k_2, k_3, and k_4 are nonnegative numbers.

Optimization of (2.4) over all $T^j_{l,k}$ ($l = \overline{0, L}$) for finding the temperature on the kth spatial line at the jth moment of time yields a system of nonlinear algebraic equations with a symmetric five-diagonal, positively defined matrix similar to that given in [15]. The system can also be solved by the method of nonmonotone sweep with iteration over the coefficients. The temperature value found at the first stage of solving IHCP is used here as the initial approximation. Using this procedure successively for all the moments of time, we determine the regularized temperature $T^j_{l,k}$ ($l = \overline{0, L}$ and $j = \overline{1, M}$) on the kth line. We then pass to the $(k-1)$th line and the calculation process is repeated until the surface temperature of the body is found. The heat flux $Q_w(\xi, t)$ in the region $\bar{D}$ is determined by the known field of temperatures. The best approximation is chosen according to the principle of residuals [15, 17]. The residual equation is solved by the method of chords.

3. Results of Numerical Calculations. The heat transfer of a spherically blunted cone with the half-opening angle $\beta = 5°$ was calculated numerically for the determining parameters from [3]: $M_\infty = 5$, $R_N = 0.0508$ m, and $P_{e0} = 3.125 \cdot 10^5$ Pa. The values of other parameters are: $U_\infty = 1600$ m/sec, $\rho_\infty = 0.131$ kg/m^3, $\gamma = 1.4$, Pr $= 0.7$, $c_p = 1024$ J/(kg $\cdot$ K), $H_{e0} = 1.536 \cdot 10^6$ m^2/sec^2, $L = 2.159 \cdot 10^{-3}$ m, $T_{\text{in}} = 288$ K, $\varepsilon = 0.7$, $\sigma = 5.67 \cdot 10^{-8}$ W/(m$^2 \cdot$ K^4), $\zeta_1 = 0.12$, $\zeta_2 = 0.165$, $\varphi = 0.1$, $(\rho v)_w = 3$ kg/(m$^2 \cdot$ sec). Copper [$\lambda = 386$ W/(m $\cdot$ K), $\rho = 8950$ kg/m^3, and $c = 376$ J/(kg $\cdot$ K) and steel ($\lambda = 20$ W/(m $\cdot$ K), $\rho = 7800$ kg/m^3, and $c = 600$ J/(kg $\cdot$ K)] are used as the shell materials.

Figures 1 and 2 show the results of the solution of DHCP. Figure 1a and b shows the distributions of the surface temperature and the heat fluxes for a flow of an impermeable copper shell (solid curves) and in the presence of regular injection $(\rho v)_w(\xi) = 3$ kg/(m$^2 \cdot$ sec) including (dashed curves) the heat flux along the body contour at different moments of time and ignoring (crosses) this flux. Curves 1–5 in Fig. 1a correspond to $t = 0$, 2, 10, 30, and 200 sec. Here curves 5 correspond to the stationary regime. In Fig. 1b, curves 1–3 correspond to the times $t = 0.1$, 2, and 10 sec. At the same time, the radiation equilibrium surface temperature $T_{w,\text{eq}}$ is shown in Figs. 1a and 2a by dot-and-dashed curves. The temperature $T_{w,\text{eq}}$ is determined from the nonlinear relation

$$q_w(\xi, t) - \varepsilon\sigma T^4_{w,\text{eq}} = 0, \tag{3.1}$$

in the absence of injection and from the condition of energy conservation at the surface with account of the stationary solution for the thin porous shell

$$q_w(\xi, t) - \varepsilon\sigma T^4_{w,\text{eq}} = (\rho v)_w c_{pg}(T_{w,\text{eq}} - T_{\text{in}}) \tag{3.2}$$

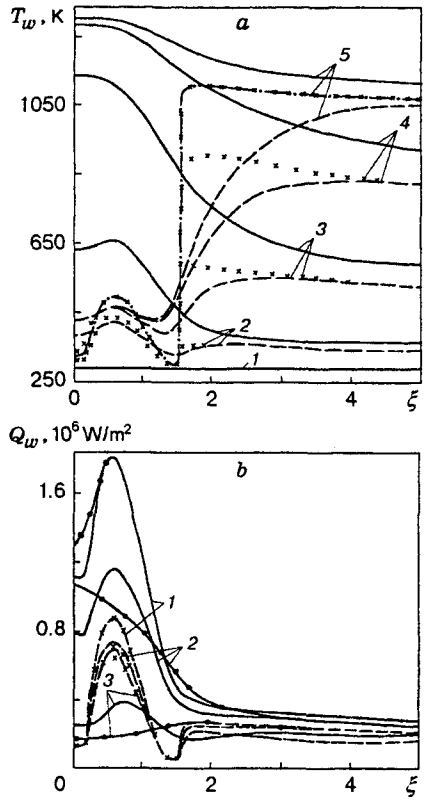

Fig. 1

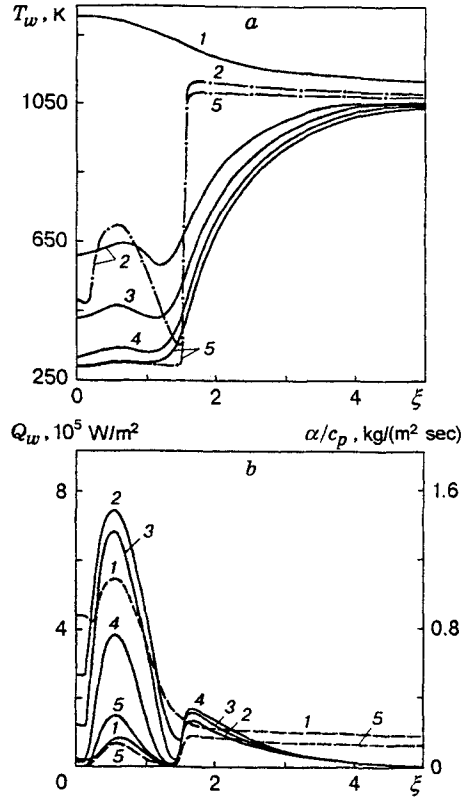

Fig. 2

in the presence of injection from a spherically blunted surface.

With the heat flux along the contour ignored, in the presence and in the absence of injection the stationary surface temperature coincides with the radiation equilibrium temperature of the surface (curves 5 in Fig. 1a), thus showing the reliability of the numerical results obtained.

As is seen from Fig. 1, the injection decreases the surface temperature and the heat flux. This decrease is the greatest in the spherically blunted region. Behind the injection section, the heat-shield regime is realized and the maximum shell temperature is attained at the conical surface. For heat-conducting materials, the shell temperature becomes uniform owing to the heat flow from the peripheral section of the cone toward the spherical bluntness. Neglect of the two-dimensional nature of heat-transfer processes in the presence of injection leads to a large difference in the surface temperatures. For example, for $t = 200$ sec and $\xi = 1.6$ this difference is approximately 530 K. On the peripheral section of the cone, the differences in the heat fluxes and the surface temperatures calculated by one- and two-dimensional mathematical models become insignificant.

Figure 2a and b shows the effect of the injection intensity on the distribution of the stationary temperature and the heat flux along the contour. Curves 1–5 correspond to $(\rho v)_w(\xi) = 0$, 1.626, 3, 6, and 10 kg/(m^2 · sec). As one should expect, the surface temperature and the heat flux decrease as the injection becomes more intense. With increase in the intensity of injection from 1.626 up to 10 kg/(m^2 · sec), the stationary surface temperature drops by about 300 K and coincides with the temperature of the injected gas in the major part of the bluntness and the heat flux becomes a factor of 5 less intense. For $(\rho v)_w(\xi) = 0$ and 10 kg/(m^2 · sec), the difference in the stationary temperatures at the spherical part reaches 1000 K. On the peripheral part of the cone, the difference between the stationary temperatures is about 50 K. The nonmonotone dependence of Q_w on the rate $(\rho v)_w$ (for example, curve 1 in Fig. 2b, which lies below the curves with account of injection) is due to the surface-temperature effect on the total heat flux. At the same time, the heat-transfer coefficient decreases monotonically depending on the injection for different cross sections ξ.

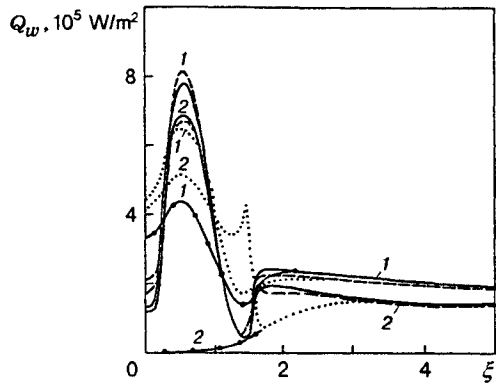

Fig. 3

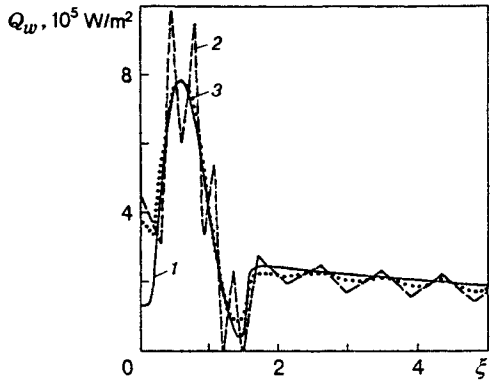

Fig. 4

Dashed curves 1 and 5 in Fig. 2b show distributions of the heat-transfer coefficients α/c_p along the generatrix ξ for $(\rho v)_w(\xi) = 0$ and 10 kg/(m^2 · sec), respectively. One can see that the injection decreases the maximum heat-transfer coefficient by almost a factor of 9 in the region of a porous spherical bluntness.

Dot-and-dashed curves 2 and 5 in Fig. 2a show the distribution of the radiation equilibrium temperature for $(\rho v)_w(\xi) = 1.626$ and 10 kg/(m^2 · sec), respectively. The maximum difference between the temperature values on the spherical part is about 400 K and insignificant on the conical part. In the heat-shield region, the temperature T_w on the conical part of the shell is much lower than the temperature $T_{w,\mathrm{eq}}$ because of the heat flux toward the peripheral part.

Figure 3 shows the results of comparison between the solutions of the IHCP (dashed and dotted curves) and the exact solution (solid curves) for $t = 1$ and 10 sec (curves 1 and 2) for the gas flow rate $(\rho v)_w(\xi) = 3$ kg/(m^2 · sec). The solution of the two-dimensional DHCP is used as the "exact" solution and the temperature of the rear surface of the shell found from the solution of DHCP is used as the initial "experimental" temperature $T_{w1}(\xi, t)$ in solving IHCP. The dotted curves show the solution of a series of one-dimensional IHCP along the body contour. Figure 3 shows that the solution of the two-dimensional IHCP (dashed curves) is stable and in good agreement with the "exact" solution. The error in determining the heat flux is approximately 4–5%, and it is less than 1% for the temperature. The heat flux Q_w obtained from the solution of one-dimensional IHCP along the body contour (dashed curves) can differ from the "exact" solution by several dozen percent with a change in the qualitative behavior near the sphere-cone joint for $\xi \approx 1.48$. An increase in the shell thickness from 2.159 to 10 mm leads to an insignificant increase in the error of $T_w(\xi, t)$ and $Q_w(\xi, t)$ from the solutions of the two-dimensional IHCP (up to 1 and 8–10%, respectively).

The problem of whether it is relevant to employ the widely used method of a thin wall [10] for determining the flux at the surface of highly heat-conductive materials with allowance for injection is studied. According to this method, the total heat flux on the wall is determined by the formula

$$Q_w(\xi, t) = q_w(\xi, t) - \varepsilon\sigma T_w^4 = \rho c L \frac{dT_w}{dt} \tag{3.3}$$

in the absence of injection and by the formula

$$Q_w(\xi, t) = \rho c L \frac{dT_w}{dt} + (\rho v)_w c_{pg}(T_w - T_g) \tag{3.4}$$

in the presence of injection. The heat flux $Q_w(\xi, t)$ calculated by formulas (3.3) and (3.4) is shown in Fig. 1b and 3 by the solid curve with points.

The numerical studies showed that, for a steel impermeable shell with low heat conductivity, the heat flux $Q_w(\xi, t)$ calculated by formula (3.3) is in good agreement (within 3–5%) with the "exact" heat flux. For a copper impermeable shell with high heat conductivity, the difference in the heat fluxes in the spherical section can exceed 50% (curves 2 and 3 in Fig. 1b). For times close to the initial moment of time, formula (3.3) gives

the largest error of determining the heat flux (curve 1 in Fig. 1b).

The calculation of the heat flux at the surface of a permeable copper shell by formula (3.4) increases the error of its determination (Fig. 3) and, for $t \geqslant 1$, the use of the formula is unreasonable. For small t, the error in determining Q_w by formula (3.4) decreases. In particular, for $t = 0.2$ sec, the error of determining the maximum heat flux is about 5–6%, which enables one to employ the method of a thin wall at moments of time close to the initial one. At the same time, the methods of solving two-dimensional IHCP enable us to recover with high accuracy the heat flux $Q_w(\xi, t)$ in the entire range of time variation of the process, which is very important, since the heat-transfer coefficient α/c_p is related to the flow conditions, the flow regime, and the geometry of the body and can depend greatly on the surface temperature and its derivative $\partial T_w/\partial\xi$ [5].

The effect of the errors of determining the initial temperature $T_{w1}(\xi, t)$ on the solution of the two-dimensional IHCP is studied. To this end, the perturbations distributed over ξ according to a sawtooth law with a deviation of 1% from the current value of temperature are superimposed on the given temperature. The numerical results showed that, in this case, the surface temperature $T_w(\xi, t)$ can be restored with an accuracy not exceeding 1–2% even if DNM are employed. At the same time, the error in determining the heat flux $Q_w(\xi, t)$ can reach 25–30%. Figure 4 shows distributions of the heat fluxes along the contour for $t = 1$ sec. Here solid curve 1 refers to the "exact" heat flux, and the dashed (2) and dotted (3) curves refer to the heat fluxes obtained from the DNM-assisted solutions of IHCP, respectively, allowing for and ignoring preliminary smoothing of the initial temperature $T_{w1}(\xi, t)$ by Tikhonov's method with the regularization parameter chosen by the method of residuals [17]. One can see that the heat-flux dependence 2 is of an unstable character, whereas the smoothing enables us to obtain a stable dependence of the heat flux that is in good agreement with the "exact" one.

With increase in the shell thickness from 2.159 up to 10 mm, the error of determining $T_w(\xi, t)$ increases up to 5% and becomes a factor of 10 greater for the heat flux. Nevertheless, the numerical calculations showed that, in this case, the employment of DNM and the smoothing of the initial temperature enabled us to obtain stable dependences of the temperature and the heat flux with errors not exceeding 5 and 20%, respectively.

Thus, solving DHCP, we have shown that the use of high-conductivity materials and injection of a gas-cooler from the surface of spherical bluntness is effective for decreasing the heat fluxes and the temperatures at the surface. A method of solving two-dimensional IHCP has been proposed and realized. This method enables one to restore the heat flux toward the body with good accuracy, whereas the methods of a thin wall and one-dimensional IHCP give a large error.

This work was supported by the Russian Foundation of Fundamental Research (Grant N. 96-01-00964).

REFERENCES

1. V. A. Bashkin and S. M. Reshet'ko, "Maximum temperature of the bluntness with allowance for heat conduction," *Uch. Zap. TsAGI*, **20**, No. 5, 53–59 (1989).
2. V. A. Bashkin and S. M. Reshet'ko, "Temperature regime of blunted wedges and cones in a supersonic flux with allowance for the heat conduction of wall material," *Uch. Zap. TsAGI*, **21**, No. 4, 11–17 (1990).
3. V. I. Zinchenko, A. G. Kataev, and A. S. Yakimov, "A study of temperature regimes of bodies in a gas flow from the surface," *Prikl. Mekh. Tekh. Fiz.*, No. 6, 57–64 (1992).
4. V. I. Zinchenko, V. I. Laeva, and T. S. Sandrykina, "Calculations of temperature regimes for bodies in flow with different thermophysical characteristics," *Prikl. Mekh. Tekh. Fiz.*, **37**, No. 5, 106–114 (1996).
5. V. I. Zinchenko, *Mathematical Modeling of Conjugate Heat- and-Mass-Transfer Problems* [in Russian], Izd. Tomsk Univ., Tomsk (1985).
6. A. M. Grishin and V. M. Fomin, *Conjugate and Unsteady Problems of the Mechanics of Reacting Media* [in Russian], Nauka, Novosibirsk (1984).
7. O. M. Alifanov, *Inverse Heat-Transfer Problems* [in Russian], Mashinostroenie, Moscow (1988).

8. A. M. Grishin, A. Ya. Kuzin, V. L. Mikov, et al., *Solution of Some Inverse Problems of the Mechanics of Reacting Media* [in Russian], Izd. Tomsk Univ., Tomsk (1987).
9. V. I. Zinchenko and A. Ya. Kuzin, "Identification of heat-transfer processes in a supersonic flow around a spherically blunted cone using the methods of solving the inverse heat-conduction problem, *Prikl. Mekh. Tekh. Fiz.*, **38**, No. 6, 105–112 (1997).
10. Yu. V. Polezhaev and F. B. Yurevich, *Thermal Protection* [in Russian], Énergiya, Moscow (1976).
11. V. N. Kharchenko, "Heat transfer in a hypersonic turbulent boundary layer upon injection of a cooling gas through a slit," *Teplofiz. Vys. Temp.*, No. 1, 101–105 (1966).
12. B. A. Zemlyanskii and G. N. Stepanov, "On heat-transfer calculation of three-dimensional hypersonic air flow around thin blunted cones," *Izv. Akad. Nauk SSSR, Mekh. Zhidk. Gaza*, No. 5, 173–177 (1981).
13. V. V. Lunev, V. G. Pavlov, and S. P. Sinchenko, "Hypersonic equilibrium dissociating air flow around a sphere," *Zh. Vychisl. Mat. Mat. Fiz.*, **6**, No. 1, 121–129 (1966).
14. A. N. Lyubimov and V. V. Rusanov, *Gas Flows Around Blunted Bodies* [in Russian], Part 2, Nauka, Moscow (1970).
15. A. Ya. Kuzin, "A regularized numerical solution of nonlinear two-dimensional inverse heat-conduction problem," *Prikl. Mekh. Tekh. Fiz.*, **36**, No. 1, 106–112 (1995).
16. Yu. S. Zav'yalov, B. I. Kvasov, and V. L. Miroshnichenko, *Methods of Spline Functions* [in Russian], Nauka, Moscow (1980).
17. O. M. Alifanov, V. K. Zantsev, B. M. Pankratov, et al., *Algorithms of Heat Flux Diagnostics on Aircraft* [in Russian], Mashinostroenie, Moscow (1983).